

Yeast Est2p Affects Telomere Length by Influencing Association of Rap1p with Telomeric Chromatin[∇]

Hong Ji, Christopher J. Adkins, Bethany R. Cartwright, and Katherine L. Friedman*

Vanderbilt University, Department of Biological Sciences, VU Station B 351634, Nashville, Tennessee 37235

Received 5 September 2007/Returned for modification 10 October 2007/Accepted 10 January 2008

In *Saccharomyces cerevisiae*, the sequence-specific binding of the negative regulator Rap1p provides a mechanism to measure telomere length: as the telomere length increases, the binding of additional Rap1p inhibits telomerase activity in cis. We provide evidence that the association of Rap1p with telomeric DNA in vivo occurs in part by sequence-independent mechanisms. Specific mutations in *EST2* (*est2-LT*) reduce the association of Rap1p with telomeric DNA in vivo. As a result, telomeres are abnormally long yet bind an amount of Rap1p equivalent to that observed at wild-type telomeres. This behavior contrasts with that of a second mutation in *EST2* (*est2-up34*) that increases bound Rap1p as expected for a strain with long telomeres. Telomere sequences are subtly altered in *est2-LT* strains, but similar changes in *est2-up34* telomeres suggest that sequence abnormalities are a consequence, not a cause, of overelongation. Indeed, *est2-LT* telomeres bind Rap1p indistinguishably from the wild type in vitro. Taken together, these results suggest that Est2p can directly or indirectly influence the binding of Rap1p to telomeric DNA, implicating telomerase in roles both upstream and downstream of Rap1p in telomere length homeostasis.

Telomeres are nucleoprotein structures that protect chromosome ends from nucleolytic digestion and preclude the recognition of normal ends as double-strand breaks (6). In most eukaryotes, telomeres are maintained by telomerase, a ribonucleoprotein that uses a short region of its RNA subunit as a template for reverse transcription. In *Saccharomyces cerevisiae*, a reverse transcriptase (RT) (*EST2*) and RNA subunit (*TLC1*) form the catalytic core of telomerase (18, 21, 35). Est2p contains at least three functional domains: an N-terminal TEN domain that anchors Est2p on its DNA substrate (23, 24) and that may interact with other protein components (10), an RNA binding (RBD) region associates with that *TLC1* RNA and contributes to dimerization (20), and an RT domain conserved among other telomerases and viral RTs (21).

While many organisms synthesize perfect TG-rich telomeric repeats, several protozoa, fungi, slime molds, and plants have heterogeneous telomere sequences (40). *S. cerevisiae* displays considerable degeneracy, with a consensus of 5'-(TG)_n-TG GGTGTG(G)_n (9). Several models have been proposed to explain this heterogeneity. An analysis of wild-type (WT) telomeres and telomeres generated in the presence of template mutations suggests that the registration of the telomere terminus occurs preferentially at the 3' end of the template, with processive synthesis through a central core region and decreasing processivity at the 5' end of the template (9, 33). In contrast, telomere junction fragments generated during chromosome healing events are more consistent with nonprocessive synthesis and patterning driven by substrate/template alignment (32). In humanized yeast cells, in which the yeast RNA template is replaced with that of

humans, Est2p generates perfect hexanucleotide repeats, suggesting that the template sequence can influence template usage (14).

In *S. cerevisiae*, the normal telomere length varies between 225 and 375 bp (43). The primary negative regulator of telomere length is Rap1p, a protein that associates directly with duplex telomeric DNA every 18 bp, on average (12). Artificially targeting Rap1p to an individual telomere proportionately shortens the TG₁₋₃ tract in cis (25, 26). This negative regulation requires Rif1p and Rif2p, proteins that bind to the C terminus of Rap1p and play overlapping, but not fully redundant, roles in telomere length homeostasis (13, 19, 41). The deletion of *RIF1* or *RIF2* increases the frequency of telomere elongation during a single cell cycle, suggesting that the Rap1p/Rif1p/Rif2p complex modulates telomerase access in a manner responsive to telomere length (39). Rap1p also mediates the silencing of genes near telomeres and has been implicated in the repression of nonhomologous end joining and telomere resection near a double-strand break (27–29).

While mutations in Est2p that abolish RT activity or disrupt complex assembly cause telomere shortening, three clusters of residues (see Fig. 1A) cause telomeres to overlengthen by up to ~100 bp when mutated. A mutation in motif E (*est2-motifE*) of the RT domain increases nucleotide addition processivity in vitro (30). In contrast, the *est2-up* mutants in the finger subdomain (motifs 1 and 2) allow telomerase to escape inhibition by Pif1p helicase (7). We previously identified four *est2-LT* (for long telomere) mutations in the N-terminal TEN domain (16) that overelongate telomeres by an unknown mechanism. Here, we demonstrate that *est2-LT* strains do not increase telomeric Rap1p association or gene silencing, as has been observed upon telomere overelongation in other genetic backgrounds. The *est2-LT* phenotype is suppressed when Rap1p length regulation is compromised, indicating that the decreased binding of Rap1p per nucleotide within *est2-LT* telomeres causes telomere overelongation. Although telomere sequences are altered in *est2-LT* strains, the association of Rap1p with these

* Corresponding author. Mailing address: Vanderbilt University, Department of Biological Sciences, 1161 21st Ave. S, Nashville, TN 37235. Phone: (615) 322-5143. Fax: (615) 343-6707. E-mail: katherine.friedman@vanderbilt.edu.

[∇] Published ahead of print on 22 January 2008.

TABLE 1. Strains used in this study

Strain	Genotype	Source or reference
GA426	<i>MATa ade2::hisG ura3-52 his3-11 leu2 trp1 can1::hisG VR::ADE2-TEL</i>	8
YKF500	GA426 <i>est2-LT^{E76K}</i>	This study
YKF501	GA426 <i>est2Δ::TRP1</i>	This study
YKF502	GA426 <i>rif2Δ::TRP1</i>	This study
YKF503	YKF501 <i>pif1Δ::Kan^r</i>	This study
YKF504	YKF501 <i>tlc1-human pKF417</i>	This study
FYBL1-23D	<i>MATα ura3Δ851 his3Δ200 trp1Δ63</i>	39
YKF510	FYBL1-23D <i>est2-LT^{E76K}</i>	This study

sequences is not detectably changed in vitro. Indeed, the same sequence alterations occur in all *est2* strains that abnormally increase telomere length. Taken together, these data provide evidence that a subset of residues in the catalytic subunit of *S. cerevisiae* telomerase modulates the association of Rap1p with telomeric DNA in vivo in a sequence-independent manner, thereby affecting the extent of telomere elongation.

MATERIALS AND METHODS

Strains and plasmids. See Table 1 for detailed strain genotypes. *est2-LT^{E76K}* (glutamic acid 76 to lysine) was integrated into GA426 and FYBL1-23D by two-step gene replacement to create YKF500 and YKF510, respectively. *EST2* was replaced with *TRP1* in GA426 by transforming a SacI-SphI fragment from pKF404-HXTRPa (*TRP1* from pRS314 cloned into the HindIII and XbaI sites of pKF404 [10]) to create YKF501. *RIF2* was replaced in GA426 with *TRP1* by using pFA6a-*TRP1* (22) as a template to create strain YKF502.

PIF1 gene disruption was accomplished in YKF501 (containing pKF410 [*proA-EST2 CEN URA3*] [16]) by transforming a PCR fragment (the primers were 5'-GTAGTTTTGTGATGCTGTTACAG-3' and 5'-GTGAGTTAGTCTCCTTTGGC-3', and the template was genomic DNA from the *pif1Δ::Kan^r* strain [Open Biosystems, Huntsville, AL]) to generate YKF503. *TLC1* was replaced with *tlc1-human* as described previously (14) in strain YKF501 (containing pKF417 [*EST2 CEN LEU2*]) to create YKF504. Following transformation with pKF410 or its mutant derivatives, colonies were screened for the loss of pKF417. Southern blotting was performed as described previously (10).

Cloning and sequencing of telomeres. (i) **Analysis of multiple cell cycles.** YKF501 bearing plasmid pKF410 was restreaked on plates containing 5-fluorouracil acid (5-FOA) and restreaked once to allow telomere shortening. After the reintroduction of pKF410 bearing WT or mutant *EST2*, transformants were restreaked three times (~75 generations). Genomic DNA was extracted by glass bead lysis (34), and telomere PCR was performed (39). After gel purification (Qiagen), products were ligated into pGEM T-Easy (Promega) according to the manufacturer's instructions. Inserts were sequenced by FASTERIS (Plan les Quates, Switzerland) using the primer M13F.

(ii) **Single-telomere extension (STEX).** A fresh GA426 *est2Δ::TRP1* colony (recipient) was grown overnight in 5 ml synthetic dextrose medium lacking tryptophan (SD-Trp). A total of 1×10^8 telomerase-deficient recipient cells were mixed with 1×10^9 cells of strain FYBL1-23D or YKF510 (donor) as described previously (39) and were incubated at 30°C for 4 h on yeast extract-peptone-dextrose plates. The mating efficiency (monitored by comparing the growth on SD-Trp [recipients and diploids] to the growth on SD-Leu-Trp [diploids only]) was nearly 100% (data not shown). Telomere PCR was performed as described above.

ChIP and dot blot assays. Chromatin immunoprecipitation (ChIP) was performed as described previously, with some modifications (38). Yeast strains were grown to an optical density at 600 nm of ~0.5 (50 ml in yeast extract-peptone-dextrose). Cross-linking was initiated with 1.4 ml 37% formaldehyde and terminated after 5 min by the addition of 2.5 ml 2.5 M glycine. Cells were pelleted and washed sequentially with HBS (50 mM HEPES, pH 7.5, 140 mM NaCl) and ChIP lysis buffer with phenylmethylsulfonyl fluoride (PMSF) (50 mM HEPES, pH 7.5, 140 mM NaCl, 1 mM EDTA, pH 8.0, 1% Igepal CA-630, 1% sodium deoxycholate, and 1 mM PMSF). Pellets were resuspended in 400 μl ChIP lysis

buffer (plus one Roche Complete mini-protease inhibitor tablet per 10 ml) and disrupted by glass bead lysis. The lysate was obtained by centrifugation, and DNA was sonicated to fragments of 500 to 1,000 bp. Sonicated lysate was cleared twice by centrifugation at $7,000 \times g$ for 2 min, and input samples (25 μl of 400 μl) were obtained. The remaining lysate was incubated on ice with 20 μl anti-Rap1p antibody (Santa Cruz Biotechnology). Samples were immunoprecipitated with 80 μl protein G Dynabeads (Invitrogen). Cross-linking was reversed by overnight incubation at 65°C, and DNA was detected by dot blot analysis. The probe was random-primed *S. cerevisiae* telomeric DNA or a random-primed PCR fragment from the *ARO1* gene (the primer sequences were 5'-TGACTG GTACTACCGTAACGGTTC-3' and 5'-GAATACCATCTGGTAATTCTGTA GTTTTGC-3'). The data analysis was described previously (36).

Analysis of telomere sequence data. The data analysis utilized newly synthesized sequences that were identified by the alignment of identical internal repeats. The frequency of GG-dinucleotide incorporation was calculated as the number of 5'-TGGGTGT sequences followed by GG divided by the total number of 5'-TGGGTGT sequences. When a core sequence overlapped with an adjacent repeat (5'-TGGGTGTGGGTGT), the 5' core (underlined) was considered to lack the GG sequence. Such overlapping core sequences generate a spacer with a value of -1. The frequency of overlapping core sequences is defined as the number of spacers in the -1 class divided by the total number of spacers. Predicted Rap1p binding sites were identified as described previously (33) with MatInspector (www.genomatix.de) using a 14-bp similarity matrix to assign confidence scores (17).

Rap1 protein expression, purification, and binding assays. Protein expression from pET28a(+)-Rap1p (XhoI-EcoRI) (11) was induced overnight in *E. coli* BL21 with 1 mM isopropyl-β-D-thiogalactopyranoside (IPTG) at 16°C. Recombinant His₆-tagged full-length Rap1p was enriched on nitrilotriacetic acid-agarose beads (Qiagen) by following the manufacturer's instructions and was purified by ion-exchange chromatography. Eluted protein was dialyzed in 20 mM Tris-HCl (pH 7.5), 50 mM NaCl, 20 mM KCl, 6% glycerol. The protein concentration was estimated by comparisons to bovine serum albumin standards.

For the gel shift assay, oligonucleotides (5'-ATATACACCCATACATTGA-3' and 5'-GTCAATGTATGGGTGTATA-3' [11]) were annealed to create a single Rap1p binding site (in boldface) and were labeled with Klenow polymerase (Roche) in the presence of [α-³²P]dCTP. A total of 100 fmol of ³²P-labeled DNA was mixed with increasing amounts of unlabeled telomeric DNA (0 to 80 fmol). A total of 400 fmol of recombinant Rap1p was added to 20 μl binding buffer [20 mM Tris-HCl (pH 7.5), 70 mM KCl, 1 mM dithiothreitol, 6% (vol/vol) glycerol, 25 μg/ml bovine serum albumin, 2.5 μg/ml poly(dG-dC), 0.1 mM EDTA], and reaction mixtures were incubated for 10 min on ice and for 20 min at room temperature. Samples were separated on 6% polyacrylamide Tris-borate-EDTA gels and quantified by a phosphorimager.

For DNase I footprinting, ³²P end-labeled telomeric sequences (100 fmol) and a 20-fold excess of recombinant Rap1p were mixed in 20 μl binding buffer, incubated on ice for 10 min, and incubated for 1 h at room temperature. Samples were incubated with 0.5 U DNase I (Promega) for 1 min, followed by the addition of 45 μl stop solution (supplied by the manufacturer). DNA was phenol-chloroform extracted and ethanol precipitated. Samples were resuspended in 5 μl formaldehyde loading buffer, separated on 10% polyacrylamide gels, and analyzed by a phosphorimager.

RESULTS

Rap1p association with *est2-LT* telomeres does not correlate with telomere length. The *est2-up* alleles were identified in a screen for mutations of *EST2* that improve the transcriptional silencing of a telomere-proximal gene (7). Increased telomere length is thought to mediate this phenotype by increasing Rap1p association and the subsequent recruitment of the histone deacetylase Sir2p (27). Given that the entire *EST2* open reading frame was subjected to mutagenesis, we were surprised that this screen failed to identify mutations in the *EST2* TEN domain. We speculated that *est2-LT* strains, despite containing longer-than-normal telomeres, do not increase telomeric silencing. Two representative *est2-LT* alleles were chosen for analysis: *est2-LT^{E76K}* and *est2-LT^{N95A}* (asparagine 95 to alanine). *est2-LT^{E76K}* causes the telomere length to increase by

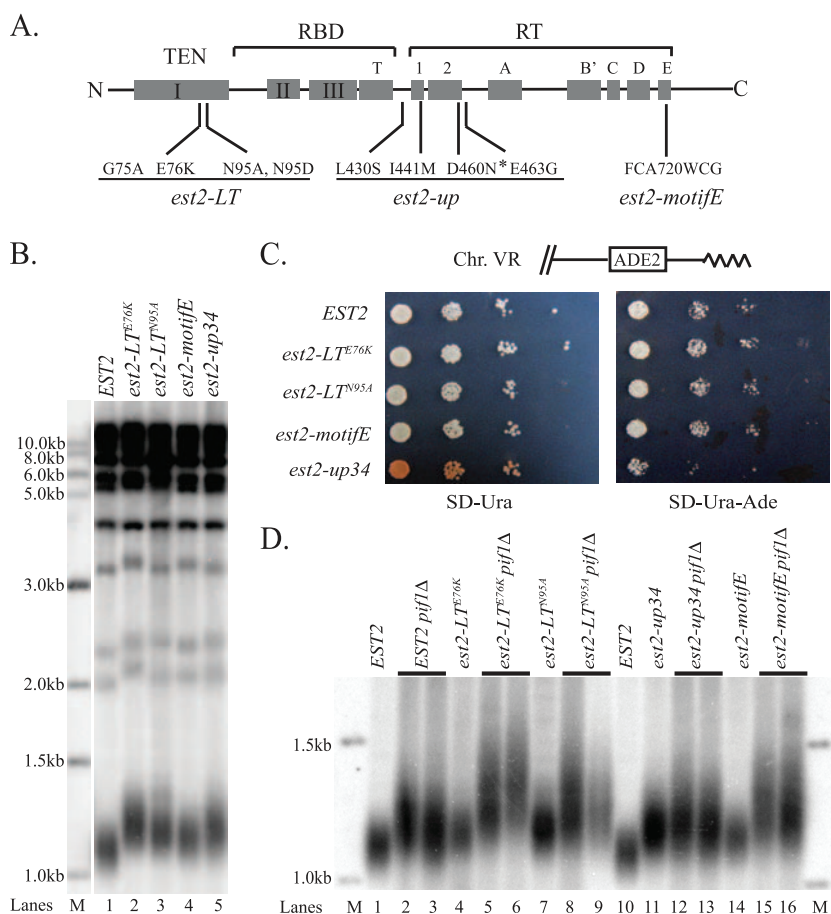


FIG. 1. Strains expressing different telomere-lengthening alleles of *EST2* have distinguishable phenotypes. (A) Locations of long-telomere mutations within *EST2*. The domain structure of Est2p is shown (15). Mutations in three distinct regions cause longer-than-normal telomeres: *est2-LT* in the TEN domain, *est2-up* in motifs 1 and 2, and *est2-MotifE* in the RT domain (7, 16, 30). The *est2-up34* allele utilized in this study (D460N) is indicated with an asterisk. (B) Telomere length in *est2* strains. Genomic DNA from the indicated strains was cleaved with *Xho*I, separated in a 1.2% agarose gel, subjected to Southern blot analysis, and probed with a telomeric DNA fragment. The strains shown are identical to those used for the silencing (C) and ChIP assays (Fig. 2). M, DNA size marker. (C) Expression of a telomere-proximal *ADE2* gene in *est2* strains. Telomeric silencing was tested in an *est2Δ ade2Δ* strain containing an ectopic copy of *ADE2* inserted near the right telomere of chromosome V (Chr. VR) (see the diagram at the top). This strain (YKF501) was transformed with a *URA3* plasmid expressing the indicated *EST2* allele. Shown are 10 \times serial dilutions of cells grown on medium lacking uracil or lacking uracil and adenine \sim 75 generations after the introduction of the complementing plasmids. (D) Dependency of *est2*-mediated telomere overlengthening on *Pif1*. Strains of genotype *est2Δ* (YKF501) and *est2Δ pif1Δ* (YKF503) were transformed with *URA3* plasmids expressing WT *EST2* (lanes 1 to 3 and 10) or the indicated *est2* allele. Cells were grown for \sim 75 generations to allow the telomere length to stabilize. Genomic DNA isolated from the indicated strains was digested with *Xho*I, subjected to Southern blot analysis, and probed with telomeric DNA. Telomeres containing a subtelomeric Y' element are shown. M, DNA size marker.

\sim 100 bp, while *est2-LT^{N95A}* has a slightly smaller, but reproducible, effect (Fig. 1B, lanes 2 and 3, respectively).

To assay telomeric gene silencing, plasmid-borne *EST2* alleles were introduced into an *est2Δ ade2Δ* strain with *ADE2* inserted near the right telomere of chromosome V (Fig. 1C). Cells expressing WT *EST2* grow well on plates lacking adenine and are predominantly white, with small red sectors indicative of moderate *ADE2* silencing (Fig. 1C). Consistently with a previous report, *est2-up34* (the *est2-up* allele with the greatest effect on telomere length [D460N]) increases telomeric silencing, as indicated by the formation of red colonies with reduced growth in the absence of adenine. In contrast, telomeric silencing in cells expressing *est2-LT^{E76K}*, *est2-LT^{N95A}*, or *est2-motifE* is indistinguishable from that of the WT (Fig. 1C). The differences in silencing behavior of the mutant strains cannot be attributed to differences

in telomere lengths, since all of them overlengthen telomeres to a similar extent (Fig. 1B). We conclude that telomere overlengthening in *est2-LT* and *est2-motifE* strains is not accompanied by increased telomeric silencing.

Given that the *est2-up* and *est2-LT* mutations differentially affect telomeric silencing and are located in distinct regions of the Est2 protein, we hypothesized that these alleles increase telomere length through distinct mechanisms. To test this hypothesis, we monitored a genetic interaction previously reported for the *est2-up* alleles. In a strain lacking the Pif1 helicase, a negative regulator of telomere length, *est2-up34* does not cause any additional telomere lengthening (7). This result, combined with biochemical evidence, suggests that mutations in the finger subdomain (including *est2-up34*) render telomerase at least partially resistant to negative regulation by Pif1p

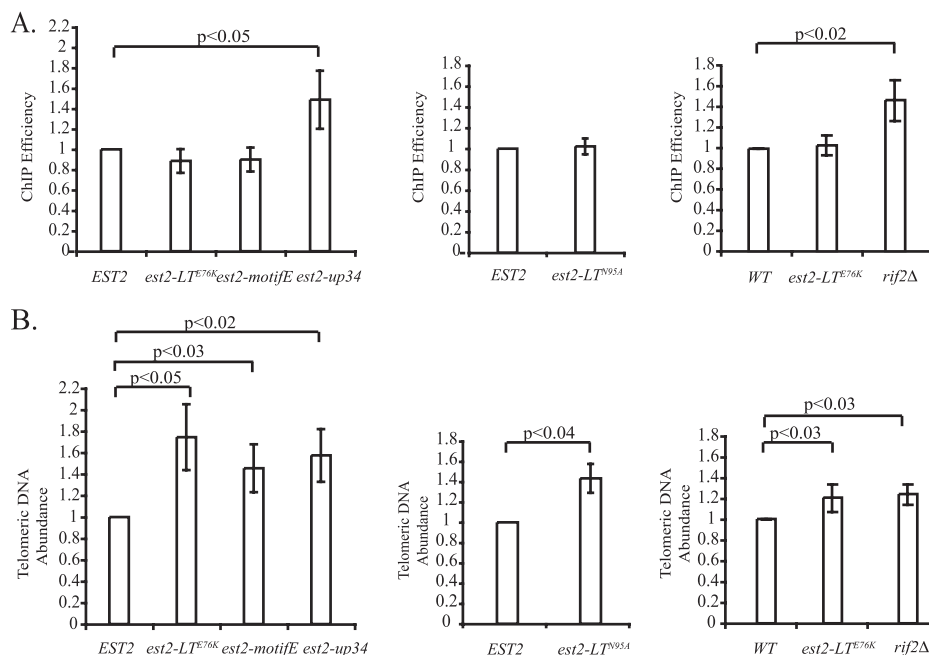


FIG. 2. Association of Rap1p with WT and mutant telomeres correlates with telomeric silencing but not with telomere length. (A) Association of Rap1p with WT and mutant telomeres. ChIP was used to measure the association of Rap1p with telomeric DNA. Values represent the fraction of total telomeric DNA immunoprecipitated with anti-Rap1p antibody normalized to the value for the WT in each independent experiment. Error bars represent standard deviations from at least three experiments. A paired *t* test was used to determine significance. *P* values are indicated (brackets) only for those samples that had values that differed significantly from those of the WT ($P < 0.05$). The left and center panels show an analysis of strains in the YKF501 (GA426 *est2Δ::TRP1*) background. The indicated *proA-EST2* alleles (WT, *est2-LT^{E76K}*, *est2-motifE*, *est2-up34*, and *est2-LT^{N95A}*) were expressed from plasmid pKF410. The strains are identical to those utilized in Fig. 1B and C. The graph on the right shows an analysis of strains in the GA426 background: GA426 (WT), YKF500 (GA426 with *est2-LT^{E76K}* integrated at the endogenous locus), and YKF502 (GA426 *rif2Δ::TRP1*). (B) Measurement of relative telomeric DNA abundance. Telomeric DNA abundance was quantified in input extracts from the samples shown in panel A by measuring the ratio of signal generated with a telomeric DNA probe to that of a single-copy sequence (a 372-bp fragment of *ARO1*). Values were normalized to those of the WT in each independent experiment. Error bars represent standard deviations from at least three experiments. A paired *t* test was used to determine significance. *P* values are indicated (brackets) for those samples that had values that differed significantly from those of the WT ($P < 0.05$).

(7). To test if other *est2* alleles behave similarly, we created a *pif1Δ est2Δ* strain expressing plasmid-borne WT or mutant alleles of *EST2*. As shown in Fig. 1D, only *est2-up34* fails to cause additional telomere lengthening in this background. We conclude that *est2-LT* and *est2-motifE* lengthen telomeres by a mechanism distinct from that of *est2-up34*.

Since Rap1p is required for telomeric silencing, our observation that increased telomere length is not always accompanied by increased gene silencing suggested that the longer telomeres of the *est2-LT* and *est2-motifE* strains do not undergo the expected increase in total Rap1p association. ChIP was used to address this possibility. To keep most telomeres intact, formaldehyde-cross-linked chromatin was sheared by sonication to 500 to 1,000 bp. Rap1p was immunoprecipitated, and the associated telomeric DNA was quantified by hybridization. To account for differences in telomere length, we expressed the amount of precipitated fragment as a percentage of the input telomeric DNA. Under these conditions, the efficiency of immunoprecipitation is proportional to the amount of Rap1p bound to each telomere. Values were normalized to those of a WT sample processed in parallel.

As predicted by the lack of increased telomeric silencing, the association of Rap1p with telomeres in *est2-LT^{E76K}*, *est2-LT^{N95A}*, and *est2-motifE* strains is indistinguishable from that

of the WT (Fig. 2A). In contrast, the expression of *est2-up34* significantly increases the efficiency of telomeric DNA immunoprecipitation by Rap1p (Fig. 2A). To rule out the possibility that *est2-up34* abnormally increases Rap1p association, we monitored a control strain (*rif2Δ*) in which the extent of telomere overelongation is similar to that observed in *est2-LT^{E76K}* and *est2-up34* strains (see below). As expected from Rif2p's role downstream of Rap1p (41), the elongated telomeres of a *rif2Δ* strain bind significantly more Rap1p than WT (Fig. 2A).

To confirm that differences in Rap1p association cannot be attributed to differences in the extent of telomere overelongation, we measured the ratio of hybridization of a telomere-specific probe to that of a single-copy control sequence (*ARO1*) in input samples from each strain. While the relative abundance of telomeric DNA was significantly increased over that of the WT, the extent of telomere overelongation in the different mutant strains was statistically indistinguishable (Fig. 2B). The observation that the longer telomeres of *est2-LT^{E76K}*, *est2-LT^{N95A}*, and *est2-motifE* strains bind no more Rap1p than do WT-length telomeres is consistent with an overall reduction (per nucleotide) in the association of Rap1p within telomeres in these mutant strains. This result led us to address the role of Rap1p in the generation of the long-telomere phenotype.

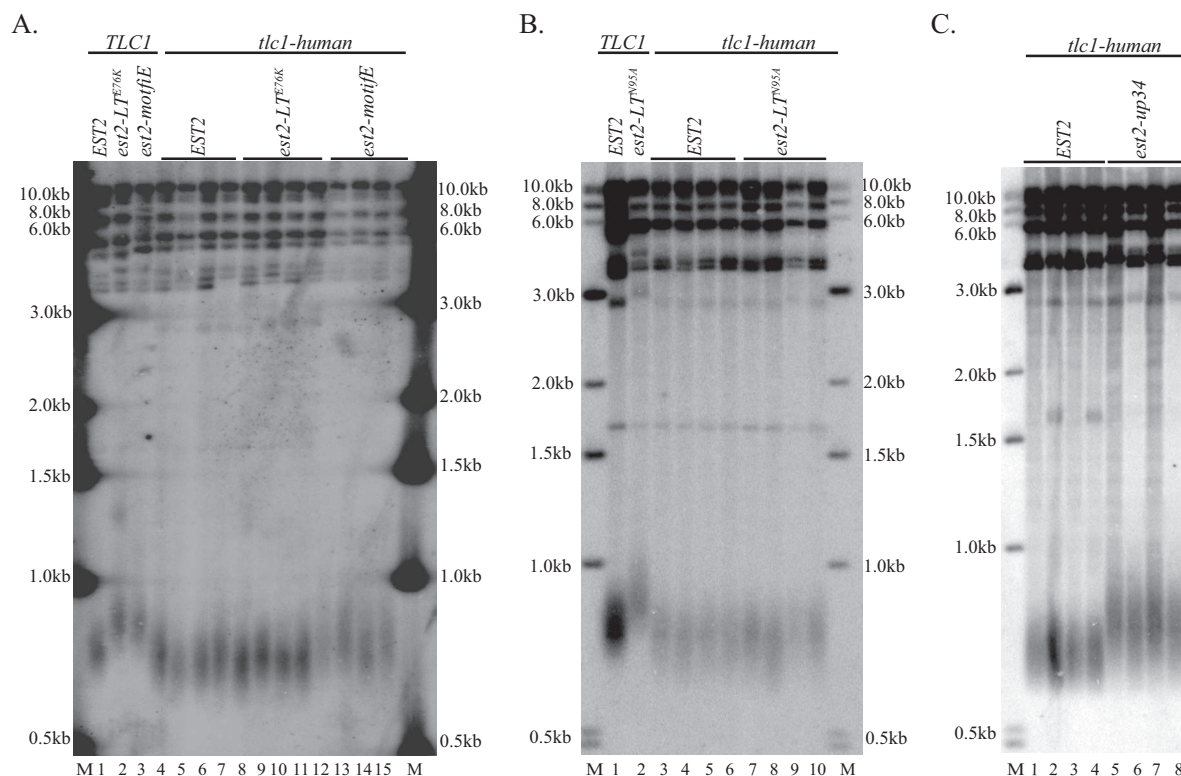


FIG. 3. Telomere overlengthening by the *est2-LT* alleles is suppressed in a background of humanized *TLC1*. (A) *est2Δ* strains expressing WT *TLC1* (lanes 1 to 3) or a *tlc1-human* variant (lanes 4 to 15) were transformed with plasmids bearing *EST2*, *est2-LT^{E76K}*, or *est2-motifE* as indicated. DNA was cleaved with *Pst*I, separated in a 1.5% agarose gel, subjected to Southern blot analysis, and probed with a mixture of two DNA fragments (*S. cerevisiae* telomere DNA and the humanized [TTAGGG]_n sequence). M, DNA size marker. (B) *est2Δ* strains expressing WT *TLC1* (lanes 1 and 2) or a *tlc1-human* variant (lanes 3 to 10) were transformed with plasmids bearing *EST2* or *est2-LT^{N95A}* as indicated. Samples were treated as described in the legend to panel A. (C) *est2Δ* strains expressing a *tlc1-human* variant were transformed with plasmids bearing *EST2* or *est2-up34* as indicated. Samples were treated as described in the legend to panel A.

Generation of the long-telomere phenotype in *est2-LT* strains requires the association of Rap1p with telomeric DNA.

Since telomere elongation is inhibited in a manner proportional to the amount of bound Rap1p, a reduction in the frequency of Rap1p association with telomeres should cause telomere overelongation (as previously observed for certain mutations in the telomerase template [31]). An equilibrium length is reached when telomeres bind, on average, an amount of Rap1p equivalent to that normally associated with WT telomeres. The observation that transcriptional silencing and total Rap1p association at the elongated telomeres of *est2-LT* and *est2-motifE* strains are equivalent to WT levels fits this prediction and suggests that telomere overlengthening is a response to reduced binding by Rap1p. If true, telomere overelongation in *est2-LT* strains should be Rap1p dependent.

We initially set out to eliminate Rap1p function by deleting its binding partners, Rif1p and Rif2p. Unfortunately, the extreme length and heterogeneity of telomeres in this background made it impossible to determine if the *est2* alleles cause additional elongation (data not shown). To circumvent this difficulty, we took advantage of a strain in which the yeast RNA template is replaced with that of the human telomerase RNA, dictating the synthesis of the hexanucleotide sequence (5'-TTAGGG) normally found at human telomeres (14). This humanized sequence does not bind Rap1p, but telomeres are

short and stable due to an alternate, Tbf1p-dependent mechanism (1, 2, 4). An *est2Δ* strain expressing the humanized *TLC1* variant (*tlc1-human*) from its endogenous locus was grown for approximately 50 generations in the absence of telomerase to allow telomere shortening. This strain subsequently was transformed with plasmids expressing WT or mutant *est2*, and telomerase was allowed to synthesize telomeres in the presence of the humanized RNA. Although the internal telomeric sequences in these strains retain WT sequence and are capable of binding Rap1p, any additional DNA synthesized by the mutant enzymes is derived from the humanized template. As one would predict for mutations dependent on Rap1p, neither *est2-LT^{N95A}* nor *est2-LT^{E76K}* increases the telomere length compared to the length of WT telomeres when the humanized RNA is used (Fig. 3A and B). In contrast, *est2-up34* retains the ability to cause telomere overlengthening in this background, which is consistent with a Rap1p-independent mode of action (Fig. 3C). Surprisingly, *est2-motifE* also overelongates telomeres in this background (Fig. 3A, lanes 12 to 15). Telomeres cloned from the *est2-LT^{E76K}* and *est2-motifE* strains contain perfect 6-nucleotide repeats at the chromosome terminus (data not shown), confirming that Rap1p binding is eliminated within the newly synthesized sequences. The failure of *est2-LT^{E76K}* and *est2-LT^{N95A}* to lengthen telomeres in the humanized background suggests that telomere lengthening oc-

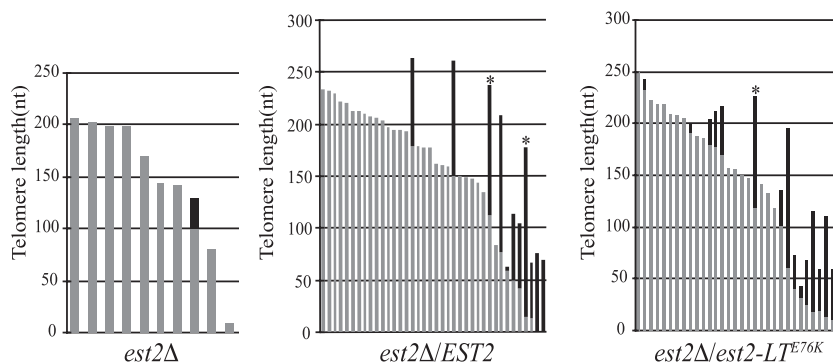


FIG. 4. Analysis of telomere addition in a single cell cycle. An *est2Δ* recipient strain was mated with strains expressing either WT *EST2* (center) or *est2-LT^{E76K}* (right). Telomeres were cloned and sequenced after the completion of the first postzygotic S phase. The lengths of individual telomeres are plotted. For each telomere, identical TG₁₋₃ sequences resulting from semiconservative DNA replication (gray) and divergent sequences representing new telomere additions (black) are shown. Based on the low frequency of telomere additions in the absence of mating (left) and on the observed significant differences in the telomere sequence following mating to an *EST2* or *est2-LT^{E76K}* donor (Table 1), we infer that most divergent sequences result from telomere extension by telomerase. The average amounts of new telomere addition are 82 (*EST2*) and 58 (*est2-LT^{E76K}*) nucleotides (nt). These differences are not statistically significant ($P = 0.084$; nonparametric Kruskal-Wallis test). Likewise, the frequency of telomere addition is statistically indistinguishable between the two strains ($P = 0.09$; Fisher's exact test). Telomeres utilized for experiments shown in Fig. 6 and 7 are indicated with asterisks.

curs in response to the reduced frequency of telomeric Rap1p association in vivo, although we cannot eliminate the possibility that altering the template sequence has other unanticipated effects on the *est2-LT* phenotype. We also conclude that *est2-motifE* affects telomere length in a manner that is at least partially Rap1p independent.

Telomere overelongation is associated with altered telomere sequences in vivo. We sought to understand the mechanism through which the frequency of Rap1p association is decreased at *est2-LT* telomeres. Given that Rap1p associates directly with telomeric DNA, altering the sequence of the telomeric repeat also could have this effect. To examine this possibility, telomere sequences were obtained in two ways that allowed the unambiguous identification of repeats synthesized by the mutant enzyme. In an analysis of telomere addition over multiple cell cycles, telomeres were allowed to shorten for ~50 generations in the absence of *EST2*. WT or mutant *EST2* was introduced, the telomere length was recovered for ~75 generations, and multiple clonal isolates of a single telomere were sequenced (9). Because yeast telomerase generates irregular sequences, repeats synthesized after the introduction of the complementing plasmid were identified by their divergence from the identical, internal repeats. In a second approach (STEX), telomere repeats generated during a single S phase were analyzed (39). *est2Δ* recipient cells with shortened telomeres were mated with donor cells expressing *EST2* or *est2-LT^{E76K}* at the endogenous locus. After zygotes proceeded through the first postzygotic S phase, marked telomeres originating in the recipient strain were cloned and sequenced. Again, newly synthesized repeats were identified as those sequences that did not align between different telomeres. The frequency and extent of telomere elongation by *est2-LT^{E76K}* telomerase during a single S phase were not statistically different from those of the WT, with a marked preference for the elongation of the shortest telomeres, as previously reported (Fig. 4) (39).

A detailed inspection of *est2-LT^{E76K}* telomeres did indeed reveal a change in the telomere sequence. As previously described, approximately 90% of repeats in WT telomeres con-

tain a 7-nucleotide core sequence (5'-TGGGTGT) (Fig. 5A), half of which are followed by two consecutive G nucleotides (as templated by *TLC1*) (9). *est2-LT^{E76K}* telomeres contain this GG dinucleotide at an increased frequency (67 to 77%) (Table 2). A combined probability test that examined the magnitude of the effect in telomeres generated by both experimental regimens indicated statistical significance ($P = 0.025$) (37).

While the majority of core sequences in WT telomeres are separated by two or more nucleotides, nearly 30% overlap to generate the sequence 5'-TGGGTGTGGGTGT (a spacing of -1). Telomeres synthesized in a single cell cycle by *Est2-LT^{E76K}* show a greater than 50% reduction in the -1 spacer class (Table 3) and an overall shift in the distribution of spacer lengths ($P = 0.03$) (Fig. 5B). This is the first reported example of a mutation within the yeast catalytic subunit that affects the patterning of telomere repeats in vivo.

To address the potential impact on Rap1p binding, a computer algorithm (MatInspector) was used to identify putative Rap1p sites in WT and mutant sequences (5). As previously described, nearly all predicted Rap1p binding sites fall into three classes corresponding to 13/13, 12/13, and 11/13 matches to the consensus sequence (33). *est2-LT^{E76K}* telomeres shift the distribution among these classes, with a relative paucity of the 5'-TGGGTGTGGGTGTG sequence (11/13 matches) reflecting the reduction in overlapping core sequences (Table 4). In addition, the extent of overlap between adjacent predicted Rap1p sites is reduced in *est2-LT^{E76K}* telomeres ($P = 0.042$) (Fig. 5C and D). This effect is small and does not decrease the total number of predicted sites across the length of a telomere. However, we speculated that changing the relative spacing of adjacent sites could disproportionately affect Rap1p occupancy.

We reasoned that if the sequence alterations observed in *est2-LT^{E76K}* telomeres directly account for the reduced frequency of Rap1p binding (Fig. 2A), similar changes should be observed in other strains that exhibit this phenotype (*est2-LT^{N95A}* and *est2-motifE*). Indeed, the sequencing of telomeres generated in both strains during multiple generations reveals

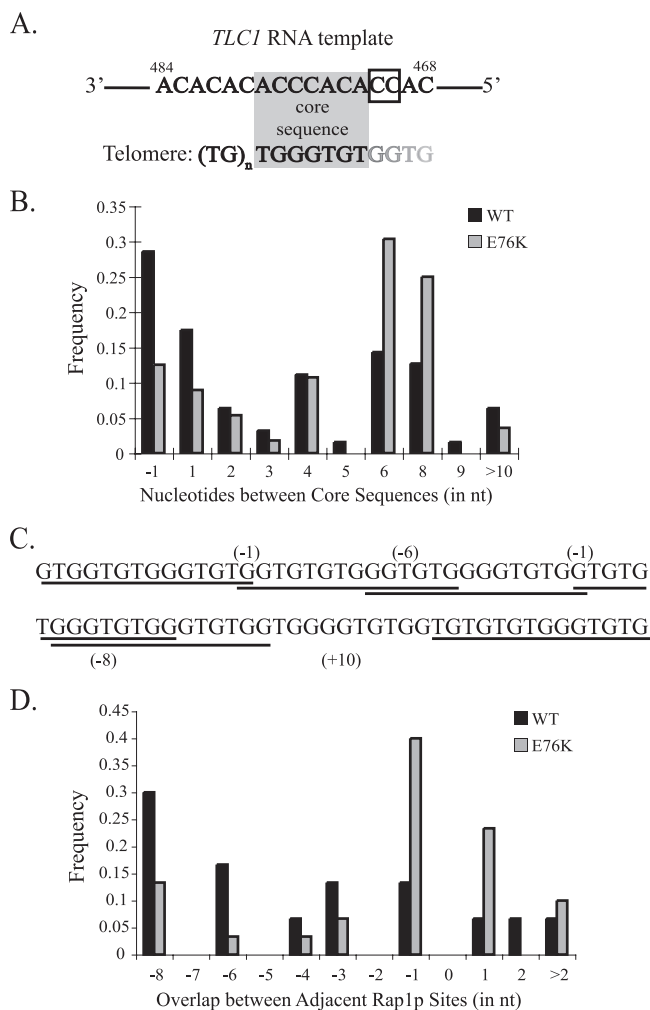


FIG. 5. Pattern of telomere repeat addition is altered in *est2-LT^{E76K}* strains. (A) Model of yeast telomere repeat heterogeneity (9). Processive reverse transcription of a central portion of the telomerase template RNA (gray) incorporates the 5'-TGGGTGT core sequence in ~90% of repeats. Heterogeneity is proposed to arise from a combination of poor processivity (gray nucleotides), multiple registers of alignment, and abortive reverse transcription at the 3' end of the template. The GG dinucleotide is produced by the reverse transcription of ⁴⁷⁰CC⁴⁷¹ (box). (B) The number of nucleotides between core sequences is significantly altered in *est2-LT^{E76K}* telomeres. The number of nucleotides between core sequences (5'-TGGGTGT) was graphed from WT and *est2-LT^{E76K}* telomeres synthesized during a single cell cycle; -1 spacing occurs when the 3' T of one core sequence is identical to the 5' T of the next. Data are derived from 65 WT repeats and 55 mutant repeats. The distributions of absolute values are statistically different ($P < 0.02$) by the chi-square contingency test. (C) The majority of predicted Rap1p binding sites overlap. Rap1p sites predicted within a representative WT sequence (see Materials and Methods) are underlined. Overlap is indicated by negative values (parentheses). (D) Predicted Rap1p binding sites are more dispersed in *est2-LT^{E76K}* telomeres than in WT telomeres. The amount of overlap between 31 predicted Rap1p binding sites in WT telomeres and 31 sites in *est2-LT^{E76K}* telomeres was determined by using the method illustrated in panel C, and the frequency of each class was plotted. Distances of greater than two nucleotides were grouped. Distributions of absolute values are statistically different ($P = 0.042$) by the chi-square contingency test. nt, nucleotide.

TABLE 2. Comparison of GG dinucleotide incorporation by WT and mutant telomerase

No. of cell cycles	% GG dinucleotide incorporation ^a				
	WT	<i>est2-LT^{E76K}</i>	<i>est2-LT^{N95A}</i>	<i>est2-motifE</i>	<i>est2-up34</i>
Multiple	52.5 (31/59)	67.1 (53/79)	63.6 (35/55)	64.9 (37/57)	65.1 (56/86)
Single	56.6 (43/76)	77.3 ^b (51/66)			

^a Calculated as the percentage of total core sequences that are followed by a GG dinucleotide (see Materials and Methods). Values in parentheses are the numbers of core sequences followed by the GG dinucleotide out of the total numbers of core sequences observed.

^b The difference between the GG dinucleotide incorporation of WT and *est2-LT^{E76K}* telomeres is significant according to a Fisher's exact test ($P = 0.012$).

sequence changes reminiscent of those observed in *est2-LT^{E76K}* (Tables 2 and 3), with similar changes in the distribution of predicted Rap1p binding sites (data not shown). As a control, we examined telomere sequences from the *est2-up34* strain. Since Rap1p binding is increased at *est2-up34* telomeres in vivo (Fig. 2A), we predicted no change in the telomere sequence. Contrary to our expectation, *est2-up34* telomeres also display an increased GG-dinucleotide frequency and a reduced amount of core sequence overlap compared to those of the WT. Indeed, the telomere sequence changes among the four mutant strains are statistically indistinguishable (Tables 2 and 3) ($P = 0.98$ and 0.87 between GG incorporation and overlapping core sequences, respectively, in a two-by-four chi-square contingency test). Given that changes in the telomere sequence do not correlate with the extent of Rap1p binding in vivo, we conclude that altered telomere patterning is a consequence, rather than a cause, of telomere overelongation in these mechanistically distinct *est2* strains.

Rap1p association at WT and *est2-LT^{E76K}* telomeres is indistinguishable in vitro. Although telomere sequence alterations do not appear to be directly responsible for reduced Rap1p binding in vivo, we wanted to determine the consequence of the predicted changes in Rap1p binding sites observed at *est2-LT^{E76K}* telomeres. To address whether these altered sequences reduce Rap1p association, we assayed the binding of recombinant Rap1p to cloned WT and mutant telomeres in vitro. Matched WT and mutant clones containing approximately the same amounts of telomeric DNA (~230 or ~180 bp) were chosen from the STEX experiment (Fig. 4). In the mutant telomeres, 91% (E184) or 48% (E229) of the total TG₁₋₃ sequence was synthesized by *est2-LT^{E76K}* telomerase. In general, sequences on these telomeres are representative of

TABLE 3. Comparison of telomere sequences added by WT and mutant telomerase

No. of cell cycles	% of overlapping core sequences ^a				
	WT	<i>est2-LT^{E76K}</i>	<i>est2-LT^{N95A}</i>	<i>est2-motifE</i>	<i>est2-up34</i>
Multiple	29.2 (14/48)	17.5 (11/63)	20.5 (9/44)	14.5 (8/55)	15.6 (12/77)
Single	27.7 (18/65)	12.7 ^b (7/55)			

^a Calculated as the percentage of adjacent core sequences that share a common nucleotide (see Materials and Methods). Values in parentheses are the numbers of adjacent pairs of core sequences in which no intervening sequence occurs out of the total number of core sequences observed.

^b Fisher's exact test was used to compare the difference between WT and *est2-LT^{E76K}* telomeres ($P = 0.07$).

TABLE 4. Predicted Rap1p binding sites in WT and *est2-LT^{E76K}* telomeres

Rap1p site	Matrix similarity ^a	No. of nucleotides matching the 13-bp consensus	% Occurrence ^b	
			WT	<i>est2-LT^{E76K}</i>
GGTGTGTGGGTGTG	0.902	13	40.0 (14/35)	47.2 (17/36)
TGTGTGTGGGTGTG	0.901	12	17.1 (6/35)	36.1 (13/36)
TGGGTGTGGGTGTG	0.806	11	25.7 (9/35)	11.1 (4/36)
GTGGTGTGGGTGTG	0.795	11	17.1 (6/35)	5.6 (2/36)

^a Rap1p sites were identified using the MatInspector program (www.genomatix.de) and a similarity matrix described previously (17). Scores reflect the strength of the match to the similarity matrix.

^b WT and *est2-LT^{E76K}* sequences derive from experiments using a single cell cycle. Percentages are rounded to one decimal place and do not sum to 100% in some cases due to rounding. The numbers in parentheses indicate the numbers of the different types of Rap1p site out of the total numbers of predicted Rap1p sites.

the overall trend of increased GG-dinucleotide incorporation and decreased core sequence overlap observed among all *est2-LT^{E76K}* telomeres (Fig. 6A). The variability in the GG-dinucleotide rate observed in the WT telomere sequences reflects the stochastic variation given the small number of repeats in each clone. Consistently with the relatively small change in overlap between predicted Rap1p binding sites that we observed among all mutant telomeres (Fig. 5C and D), the total number of predicted Rap1p binding sites is similar between size-matched WT and *est2-LT^{E76K}* telomere clones (Fig. 6A).

To address the occupancy of predicted Rap1p sites, we monitored the binding of full-length, recombinant Rap1p to WT and *est2-LT^{E76K}*-derived sequences by DNase I footprinting. In all four telomeres, regions of protection correspond well with our predictions (Fig. 6B). The strong protection observed on *est2-LT^{E76K}* telomeres suggests that the majority of substrates are bound, arguing against a substantial decrease in binding efficiency.

To quantify Rap1p association more carefully, we measured the ability of the size-matched WT and *est2-LT^{E76K}* telomeres to compete for Rap1p binding to a short double-stranded substrate by gel shifting. Unlabeled telomeric competitor DNA quantitatively reduces the association of Rap1p with the radio-labeled substrate (Fig. 7A). Because each unlabeled DNA contains 14 to 17 potential Rap1p binding sites (Fig. 6A), effective competition occurs at low molar ratios. This assay is quite sensitive, as we could distinguish between two WT telomere sequences differing by less than 30% in length (239 bp versus 178 bp) (Fig. 7B). The ability of the longer sequence to compete for nearly half of the binding to the short oligonucleotide at a 1/20 molar ratio suggests that most or all of the 16 predicted Rap1p sites on this fragment are bound by Rap1p. *est2-LT^{E76K}* telomeres compete at least as well for Rap1p binding as their size-matched controls. For example, at the 1/20 molar ratio, *est2-LT^{E76K}* and WT telomeres of ~180 bp reduce the shifted product by 25.5% ± 1.5% and 18.9% ± 10.2%, respectively. The longer *est2-LT^{E76K}* telomere (E229) competes even better than its WT counterpart, perhaps reflecting the additional Rap1p site predicted within this sequence (Fig. 6A). We conclude that changes in the telomere sequence can-

not account for the reduced frequency with which Rap1p associates with *est2-LT* telomeres in vivo.

DISCUSSION

Telomerase negatively influences telomere length through three distinct mechanisms corresponding to the three classes of *est2* mutations that overelongate telomeres (7, 16, 30, and this work). Unexpectedly, some of these mutants (*est2-LT* and *est2-*

A.

	Percent of GG dinucleotide (values)	Percent of overlapping core sequences(values)	Predicted Rap1p sites
W239	45 (9/20)	26.3 (5/19)	16
E229	63.2 (12/19)	16.7(3/18)	17
W178	64.3 (9/14)	30.8 (4/13)	14
E184	83.3 (10/12)	10 (1/10)	14

B.

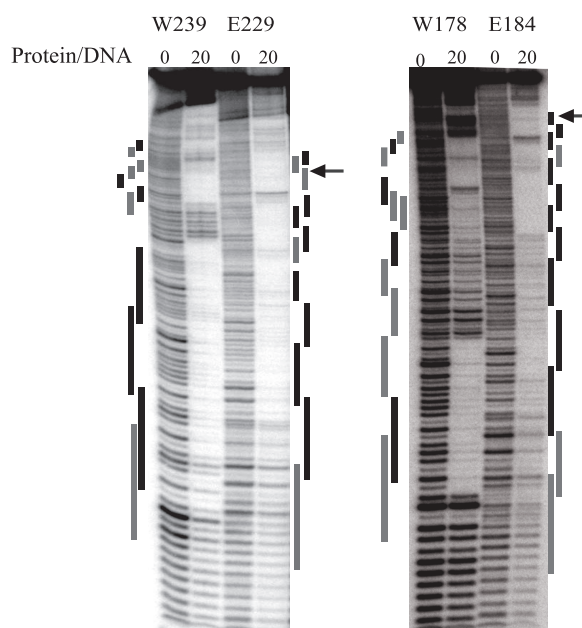


FIG. 6. *est2-LT^{E76K}* telomeres bind Rap1p at predicted sites in vitro. (A) The characteristics of four cloned telomere fragments utilized in panel B and Fig. 7 are shown. Two WT telomeres (W239 and W178) and two *est2-LT^{E76K}* telomeres (E229 and E184) were generated by telomere addition in a single cell cycle. Numbers indicate the lengths of the TG₁₋₃ repeats. In *est2-LT^{E76K}* telomeres, only a portion of this sequence is generated by the mutant enzyme (91% for E184 and 48% for E229). The percentage of core sequences followed by GG, the percentage of overlapping core sequences, and the number of predicted Rap1p binding sites (see Materials and Methods) were determined for the entire TG₁₋₃ sequence. Each DNA fragment also contains ~100 bp of identical subtelomeric and vector-derived sequences. (B) DNase I footprinting analysis of Rap1p bound to telomeric substrates. Rap1p (20-fold molar excess) was bound to 100 fmol of ³²P end-labeled telomeric DNA (W239, W178, E229, or E184 as indicated) prior to DNase I treatment. Control reaction mixtures (0) were incubated in the absence of Rap1p. A black bar indicates a 13/13 or 12/13 match to the Rap1p consensus sequence, and a gray bar indicates an 11/13 match (see Materials and Methods and Table 4). Not all Rap1p sites are shown due to the poor resolution near the top of the gel. For E229 and E184, the transition between sequences synthesized by *est2-LT^{E76K}* telomerase (at the labeled end of the DNA molecule) and the WT telomerase is indicated (arrow).

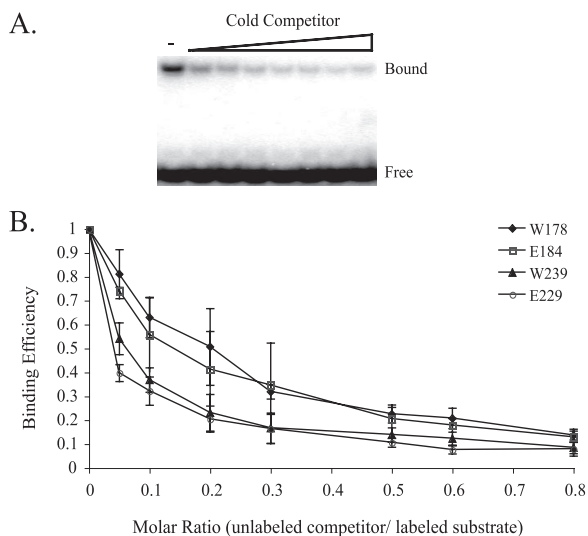


FIG. 7. Association of Rap1p with *est2-LT^{E76K}* telomeres is not reduced in vitro. (A) Increasing amounts (0, 5, 10, 20, 30, 50, 60, and 80 fmol) of WT (W239) unlabeled telomeric DNA were mixed with 100 fmol of an 18-bp ³²P-labeled double-stranded DNA and 400 fmol of recombinant Rap1p. Binding reactions were separated by polyacrylamide gel electrophoresis and visualized by a phosphorimager. (B) Quantification of multiple experiments performed as described for panel A using WT (W239 and W178) or mutant (E229 and E184) competitor DNAs. The percent competition was calculated by normalizing the fraction of oligonucleotide bound to Rap1p in each sample to the value observed in the absence of competitor. Error bars represent standard deviations from three independent experiments.

motifE) decrease the frequency of Rap1p association with telomeric chromatin in vivo. While overelongation is accompanied by changes in the telomere sequence, such alterations are not restricted to strains in which Rap1p binding is reduced and do not decrease the binding of Rap1p to telomeric DNA in vitro. These data provide evidence that the catalytic subunit of telomerase directly or indirectly influences the association of Rap1p with telomeric DNA in a manner that is independent of the telomere sequence, suggesting that telomerase plays roles upstream and downstream of Rap1p in the regulation of telomere length.

Mechanisms of telomere overelongation by *est2* alleles. Previous studies identified telomere-overelongating mutations in three regions of *EST2*. The *est2-up* mutations in the finger subdomain alter the interaction of Est2p with Pif1p (7), a helicase that disrupts the association of telomerase with its DNA substrate (3). In contrast to the *est2-up* mutations, both *est2-LT* alleles tested here cause additional telomere lengthening in the absence of *PIF1* (Fig. 1D), indicating that these mutant proteins preserve normal interactions with Pif1p. Differential effects of *est2-up34* and the *est2-LT* mutations on Rap1p association with telomeric DNA in vivo underscore this distinction (Fig. 2).

The mechanism of telomere overelongation by the *est2-motifE* allele is more complex. This mutation mimics the viral consensus sequence within motif E of the RT domain and increases the nucleotide addition processivity in vitro (30), a phenotype not shared by *est2-LT^{E76K}* or *est2-LT^{N95A}* (16). Despite this difference, *est2-motifE* decreases Rap1p association with telomeres in vivo in a manner indistinguishable from that

of *est2-LT^{E76K}* (Fig. 2). However, the persistence of the *est2-motifE* long-telomere phenotype in the absence of Rap1p association (Fig. 3A) suggests that altered enzymatic activity contributes to telomere overelongation.

Generation of abnormal sequences in long-telomere strains.

The properties of yeast telomerase that influence the telomere sequence in vivo are poorly understood. A previous study revealed normal sequences in strains with short but stable telomeres (*tel1Δ* and *ku70Δ*) (33). For the first time, we report a consistent change in the telomere sequence in *est2* strains with long telomeres. The ubiquity of this effect suggests that the telomerase activity is altered under conditions of overelongation. Alternatively, each *est2* mutation may similarly affect telomerase catalysis in vivo, despite increasing the telomere length through genetically distinct pathways. The *est2-LT^{E76K}* mutation increases repeat addition processivity of telomerase on certain primers in vitro (24). However, our observation that the number of nucleotides added per telomere-lengthening event is not increased in this mutant (an average of 82 nucleotides in the WT versus 58 nucleotides in the *est2-LT^{E76K}* strain; $P = 0.084$) (Fig. 4) suggests that this effect does not contribute to telomere overelongation in vivo.

The most obvious explanation for increased GG-dinucleotide incorporation is an increased propensity of telomerase to reach the end of the template before dissociating or translocating. We addressed this possibility by using an RNA template mutant containing a U at position 469 (Fig. 5A) (9). WT and *est2-LT^{E76K}* strains incorporate the complementary A at indistinguishable rates (10.6 and 9.9% of total repeats, respectively). Therefore, any change in nucleotide addition processivity is restricted to template residue C⁴⁷⁰. This interpretation assumes that excess GG dinucleotides are templated by residues ⁴⁷¹CC⁴⁷⁰, as previously demonstrated for the WT (9). Indeed, a mutation that eliminates the templating CC dinucleotide (⁴⁷²CAC⁴⁷¹ to ACA) abolishes GG dinucleotides in *est2-LT^{E76K}* telomeres (data not shown). Taken together, these observations are inconsistent with large changes in nucleotide addition processivity. We propose that the spectrum of permitted primer/template alignments is altered under conditions in which the normal negative regulation of the telomere length is compromised.

Association of Rap1p with telomeres in vivo. We were surprised to discover that *est2-LT* and *est2-motifE* strains do not increase Rap1p association with telomeres in vivo, despite increasing the telomere length by ~30%. The failure to detect this increase is not an experimental limitation, since *est2-up34* and *rif2Δ* strains similarly overlengthen telomeres but significantly increase the immunoprecipitation of telomeric DNA with Rap1p (Fig. 2). We hypothesize that telomere overelongation in an *est2-LT^{E76K}* strain is a response to reduced Rap1p association, since lengthening is not observed when Rap1p's regulatory function is bypassed in the humanized strain (Fig. 3). We cannot exclude the possibility that the increased processivity of Est2-LT^{E76K}p contributes to telomere overelongation (and is suppressed by the humanized *TLC1* template). However, a model in which reduced Rap1p association causes telomere lengthening is consistent with our previous observation that the expression of the *est2-LT^{E76K}* phenotype requires Tel1p, a downstream effector of the Rap1p pathway (16). Furthermore, this model also explains the lack of significant

changes in the frequency or extent of telomere addition by *est2-LT^{E76K}* telomerase in a single cell cycle (Fig. 4), since the telomeric substrates undergoing elongation have not previously encountered the mutant enzyme and are expected to bind Rap1p normally.

What accounts for the reduced association of Rap1p with *est2-LT* and *est2-motifE* telomeres in vivo? Our original hypothesis, that Rap1p binding is reduced by changes in the telomere sequence, is inconsistent with the observation that *est2-up34* telomerase generates similarly altered telomere sequences but increases overall Rap1p association in vivo. Furthermore, sequences generated by *est2-LT^{E76K}* telomerase bind recombinant Rap1p at least as well as the WT in vitro (Fig. 7). Conflicts between our observations can be reconciled if a mechanism independent of the DNA sequence influences Rap1p association with telomeres in vivo. One possibility is that telomerase, either directly or indirectly, promotes the loading of Rap1p onto newly synthesized terminal sequences. Upon the reduction of this activity in *est2-LT* strains, telomeres continue to elongate until Rap1p binds at a level equivalent to that found at normal-length telomeres. In this light, it is interesting that several subunits of the INO80 chromatin-remodeling complex recently have been shown to negatively regulate telomere length, perhaps through a physical interaction with the telomerase complex (42). Therefore, telomerase may participate in the normal formation of telomeric chromatin. The identification of other long-telomere strains that fail to increase Rap1p association will address these intriguing possibilities.

ACKNOWLEDGMENTS

We thank V. Zakian, J. Lingner, T. Weil, P. Liu, and K. Runge for generous gifts of protocols and reagents; D. McCauley for help with statistical analysis; D. Kaplan, T. Graham, E. Fanning, and X. Jiang for helpful suggestions and reagents; and J. Talley for help in protein purification. We appreciate critical comments on the manuscript from R. Bairley and M. Platts. We are grateful to the anonymous reviewers for helpful comments and suggestions.

This work was supported by American Cancer Society Research Scholar grant RSG-04-048-GMC and National Science Foundation grant MCB-0721595 to K.L.F., grant no. 52003905 of the Howard Hughes Medical Institute Professors Program, and a Dissertation Enhancement Grant from Vanderbilt University to H.J.

REFERENCES

- Alexander, M. K., and V. A. Zakian. 2003. Rap1p telomere association is not required for mitotic stability of a C(3)TA(2) telomere in yeast. *EMBO J.* **22**:1688–1696.
- Berthiau, A. S., K. Yankulov, A. Bah, E. Revardel, P. Luciano, R. J. Wellinger, V. Geli, and E. Gilson. 2006. Subtelomeric proteins negatively regulate telomere elongation in budding yeast. *EMBO J.* **25**:846–856.
- Boulé, J. B., L. R. Vega, and V. A. Zakian. 2005. The yeast Pif1p helicase removes telomerase from telomeric DNA. *Nature* **438**:57–61.
- Brevet, V., A. S. Berthiau, L. Civitelli, P. Donini, V. Schramke, V. Geli, R. Ascenzioni, and E. Gilson. 2003. The number of vertebrate repeats can be regulated at yeast telomeres by Rap1-independent mechanisms. *EMBO J.* **22**:1697–1706.
- Cartharius, K., K. Frech, K. Grote, B. Klocke, M. Haltmeier, A. Klingenhoff, M. Frisch, M. Bayerlein, and T. Werner. 2005. MatInspector and beyond: promoter analysis based on transcription factor binding sites. *Bioinformatics* **21**:2933–2942.
- de Lange, T., E. H. Blackburn, and V. Lundblad (ed.). 2006. *Telomeres*, 2nd ed. Cold Spring Harbor Laboratory Press, Cold Spring Harbor, NY.
- Eugster, A., C. Lanzuolo, M. Bonneton, P. Luciano, A. Pollice, J. F. Pulitzer, E. Stegberg, A. S. Berthiau, K. Forstemann, Y. Corda, J. Lingner, V. Geli, and E. Gilson. 2006. The finger subdomain of yeast telomerase cooperates with Pif1p to limit telomere elongation. *Nat. Struct. Mol. Biol.* **13**:734–739.
- Forstemann, K., M. Hoss, and J. Lingner. 2000. Telomerase-dependent repeat divergence at the 3' ends of yeast telomeres. *Nucleic Acids Res.* **28**:2690–2694.
- Forstemann, K., and J. Lingner. 2001. Molecular basis for telomere repeat divergence in budding yeast. *Mol. Cell. Biol.* **21**:7277–7286.
- Friedman, K. L., J. J. Heit, D. Long, and T. R. Cech. 2003. N-terminal domain of yeast telomerase reverse transcriptase: recruitment of Est3p to the telomerase complex. *Mol. Biol. Cell* **14**:1–13.
- Garbett, K. A., M. K. Tripathi, B. Cencki, J. H. Layer, and P. A. Weil. 2007. Yeast TFIIID serves as a coactivator for Rap1p by direct protein-protein interaction. *Mol. Cell. Biol.* **27**:297–311.
- Gilson, E., T. Laroche, and S. M. Gasser. 1993. Telomeres and the functional architecture of the nucleus. *Trends Cell Biol.* **3**:128–134.
- Hardy, C. F. J., L. Sussel, and D. Shore. 1992. A *RAP1*-interacting protein involved in transcriptional silencing and telomere length regulation. *Genes Dev.* **6**:801–814.
- Henning, K. A., N. Moskowitz, M. A. Ashlock, and P. P. Liu. 1998. Humanizing the yeast telomerase template. *Proc. Natl. Acad. Sci. USA* **95**:5667–5671.
- Jacobs, S. A., E. R. Podell, and T. R. Cech. 2006. Crystal structure of the essential N-terminal domain of telomerase reverse transcriptase. *Nat. Struct. Mol. Biol.* **13**:218–225.
- Ji, H., M. H. Platts, L. M. Dharamsi, and K. L. Friedman. 2005. Regulation of telomere length by an N-terminal region of the yeast telomerase reverse transcriptase. *Mol. Cell. Biol.* **25**:9103–9114.
- Lascaris, R. F., W. H. Mager, and R. J. Planta. 1999. DNA-binding requirements of the yeast protein Rap1p as selected in silico from ribosomal protein gene promoter sequences. *Bioinformatics* **15**:267–277.
- Lendvay, T. S., D. K. Morris, J. Sah, B. Balasubramanian, and V. Lundblad. 1996. Senescence mutants of *Saccharomyces cerevisiae* with a defect in telomere replication identify three additional *EST* genes. *Genetics* **144**:1399–1412.
- Levy, D. L., and E. H. Blackburn. 2004. Counting of Rif1p and Rif2p on *Saccharomyces cerevisiae* telomeres regulates telomere length. *Mol. Cell. Biol.* **24**:10857–10867.
- Lin, J., and E. H. Blackburn. 2004. Nucleolar protein PinX1p regulates telomerase by sequestering its protein catalytic subunit in an inactive complex lacking telomerase RNA. *Genes Dev.* **18**:387–396.
- Lingner, J., T. R. Hughes, A. Shevchenko, M. Mann, V. Lundblad, and T. R. Cech. 1997. Reverse transcriptase motifs in the catalytic subunit of telomerase. *Science* **276**:561–567.
- Longtine, M. S., A. McKenzie III, D. J. Demarini, N. G. Shah, A. Wach, A. Brachat, P. Philippsen, and J. R. Pringle. 1998. Additional modules for versatile and economical PCR-based gene deletion and modification in *Saccharomyces cerevisiae*. *Yeast* **14**:953–961.
- Lue, N. F. 2005. A physical and functional constituent of telomerase anchor site. *J. Biol. Chem.* **280**:26586–26591.
- Lue, N. F., and Z. Li. 2007. Modeling and structure function analysis of the putative anchor site of yeast telomerase. *Nucleic Acids Res.* **35**:5213–5222.
- Marcand, S., V. Brevet, and E. Gilson. 1999. Progressive *cis*-inhibition of telomerase upon telomere elongation. *EMBO J.* **18**:3509–3519.
- Marcand, S., E. Gilson, and D. Shore. 1997. A protein-counting mechanism for telomere length regulation in yeast. *Science* **275**:986–990.
- Moretti, P., and D. Shore. 2001. Multiple interactions in Sir protein recruitment by Rap1p at silencers and telomeres in yeast. *Mol. Cell. Biol.* **21**:8082–8094.
- Negrini, S., V. Ribaud, A. Bianchi, and D. Shore. 2007. DNA breaks are masked by multiple Rap1 binding in yeast: implications for telomere capping and telomerase regulation. *Genes Dev.* **21**:292–302.
- Pardo, B., and S. Marcand. 2005. Rap1 prevents telomere fusions by non-homologous end joining. *EMBO J.* **24**:3117–3127.
- Peng, Y., I. S. Mian, and N. F. Lue. 2001. Analysis of telomerase processivity: mechanistic similarity to HIV-1 reverse transcriptase and role in telomere maintenance. *Mol. Cell* **7**:1201–1211.
- Prescott, J. C., and E. H. Blackburn. 2000. Telomerase RNA template mutations reveal sequence-specific requirements for the activation and repression of telomerase action at telomeres. *Mol. Cell. Biol.* **20**:2941–2948.
- Putnam, C. D., V. Pennaneach, and R. D. Kolodner. 2004. Chromosome healing through terminal deletions generated by de novo telomere additions in *Saccharomyces cerevisiae*. *Proc. Natl. Acad. Sci. USA* **101**:13262–13267.
- Ray, A., and K. W. Runge. 2001. Yeast telomerase appears to frequently copy the entire template in vivo. *Nucleic Acids Res.* **29**:2382–2394.
- Rose, M. D., F. Winston, and P. Hieter. 1990. *Methods in yeast genetics: a laboratory course manual*. Cold Spring Harbor Laboratory Press, Cold Spring Harbor, NY.
- Singer, M. S., and D. E. Gottschling. 1994. *TLC1*: template RNA component of *Saccharomyces cerevisiae* telomerase. *Science* **266**:404–409.
- Smith, C. D., D. L. Smith, J. L. DeRisi, and E. H. Blackburn. 2003. Telomeric protein distributions and remodeling through the cell cycle in *Saccharomyces cerevisiae*. *Mol. Biol. Cell* **14**:556–570.

37. Sokal, R. R., and F. J. Rohlf. 1995. *Biometry*, 3rd ed. Freeman and Co., New York, NY.
38. Taggart, A. K. P., S.-C. Teng, and V. A. Zakian. 2002. Est1p as a cell cycle-regulated activator of telomere-bound telomerase. *Science* **297**:1023–1026.
39. Teixeira, M. T., M. Arneric, P. Sperisen, and J. Lingner. 2004. Telomere length homeostasis is achieved via a switch between telomerase-extendible and -nonextendible states. *Cell* **117**:323–335.
40. Wellinger, R. J., and D. Sen. 1997. The DNA structures at the ends of eukaryotic chromosomes. *Eur. J. Cancer* **33**:735–749.
41. Wotton, D., and D. Shore. 1997. A novel Rap1p-interacting factor, Rif2p, cooperates with Rif1p to regulate telomere length in *Saccharomyces cerevisiae*. *Genes Dev.* **11**:748–760.
42. Yu, E. Y., O. Steinberg-Neifach, A. T. Dandjinou, F. Kang, A. J. Morrison, X. Shen, and N. F. Lue. 2007. Regulation of telomere structure and functions by subunits of the INO80 chromatin remodeling complex. *Mol. Cell. Biol.* **27**:5639–5649.
43. Zakian, V. A. 1995. Telomeres: beginning to understand the end. *Science* **270**:1601–1607.